

# QUASI-ISOCRONOUS CONDITIONS AND HIGH ORDER TERMS OF MOMENTUM COMPACTION FACTOR AT THE COMPACT STORAGE RING

A. I. Papash<sup>†</sup>, M. Fuchs, A.-S. Müller, R. Ruprecht,  
Karlsruhe Institute of Technology, Karlsruhe, Germany

## Abstract

The compact storage ring project for accelerator research and technology (cSTART) is realized at the Institute for Beam Physics and Technology of the Karlsruhe Institute of Technology (KIT). Flexible lattice of a ring benefits variety of operation modes. Different physical experiments including direct injection and circulation of Laser Plasma Accelerator (LPA) electrons are planned at cSTART. Deep variation of momentum compaction factor with simultaneous control of high order terms of alpha would demonstrate the capture and storage of ultra-short bunches of electrons in a circular accelerator. Computer studies of linear and non-linear beam dynamics were performed with an objective to estimate arrangement and performance of dedicated three pole chicanes magnets to provide quasi-isochronous conditions for electrons. Additional families of so called “longitudinal” sextupoles and octupoles were added in a ring model to control slope and curvature of momentum compaction factor as function of energy offset of particles in a bunch.

## INTRODUCTION

Special technics are applied to reduce the bunch length in electron storage rings [1, 2]. In the so-called “squeezed” operation mode, the high degree of spatial compression of the optics with reduced momentum compaction factor (“low- $\alpha$  optics”) entails complex longitudinal dynamics of the electron bunches. Bunch compression theory is based on non-linear longitudinal beam dynamics including high order terms of momentum compaction factor [3].

The path length variation of beam orbit in a ring is, up to the third order of energy deviation  $\delta$  of particles in a bunch, defined as [4, 5]

$$\Delta L(\delta) = \alpha_1 \delta + \alpha_2 \delta^2 + \alpha_3 \delta^3 \quad (1)$$

The momentum compaction factor itself depends on energy offset. High order components of the momentum compaction factor depend on dispersion function terms [6]

$$\alpha_1 = \frac{1}{L_0} \oint \left( \frac{D_0}{\rho} ds \right). \quad (2)$$

$$\alpha_2 = \frac{1}{L_0} \left[ \oint \left( \frac{D_0^2}{2\rho^2} + \frac{D_1}{\rho} + \frac{D_1'^2}{2} \right) ds \right]. \quad (3)$$

$$\alpha_3 = \frac{1}{L_0} \left[ \oint \left( \frac{D_0 D_1}{\rho^2} + \frac{D_2}{2\rho} + D_1' D_1' \right) ds \right]. \quad (4)$$

Zero current bunch length  $\sigma_l$  given by expression

$$\sigma_l = L_0 \beta_0 \delta_p \sqrt{\frac{E_0 \alpha_1}{2\pi h e U_{RF} (-\cos\varphi_s)}}. \quad (5)$$

is proportional to square root of momentum compaction factor  $\alpha_1$  and can be essentially reduced by implying low- $\alpha$  optics [7, 8].

The synchrotron tune,  $F_s$ , is a function of linear and high order terms of the momentum compaction factor [4], where  $\alpha$  can be defined as a derivative of the relative orbit lengthening with momentum offset  $\alpha = \partial(\Delta L/L_0)/\partial\delta$  [9, 10]

$$F_s(\delta) = F_0 \sqrt{\frac{h \cdot e U_{rf} (-\cos\varphi_s)}{2\pi \beta_0^2 E_0}} \cdot \sqrt{(\alpha_1 + 2\alpha_2 \delta + 3\alpha_3 \delta^2)}. \quad (6)$$

## COMPUTER MODEL OF A RING

The cSTART ring has a four-fold symmetry [11, 12] and will operate at an energy range from 40 to 90 MeV. Our computer model of a ring including magnetic elements (Fig. 1) was described in details elsewhere [13, 14].

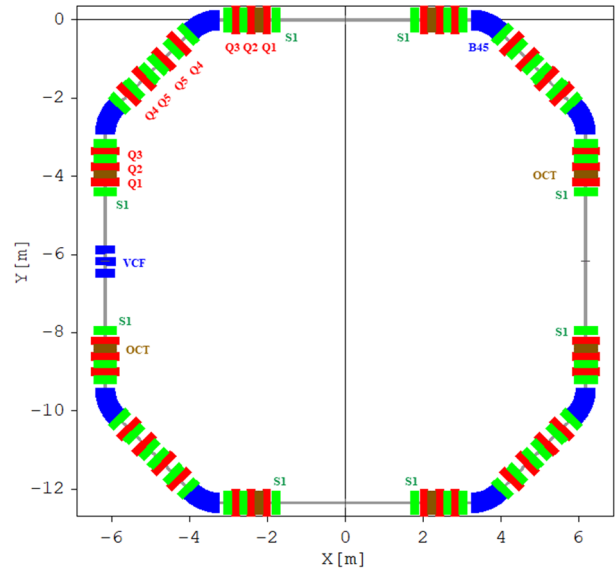


Figure 1: Computer model of the cSTART ring including variable compaction factor (VCF) magnets [14]. Dipoles B45 are depicted in blue, five families of quadrupoles Q1 to Q5 are marked in red and six families of sextupoles – in green. Family of dedicated S1 sextupoles suppresses longitudinal chromaticity while eight octupoles OCT marked in brown should control curvature of  $\alpha$  [15].

<sup>†</sup> alexander.papash@kit.edu

Family of S1 sextupoles would reduce longitudinal chromaticity (second term  $\alpha_2$ ) while octupoles should control third term  $\alpha_3$ , i.e. curvature of momentum compaction factor [15]. Three out of four straight sections of modular type are reserved for different physical experiments to pursue accelerator research and development (ARD) program at cSTART.

The synchrotron radiation (SR) damping is extremely weak at low energies. Damping time exceeds 30 s at 50 MeV and it is reduced to 4 s at 90 MeV. Ring will operate at non-equilibrium conditions. R&D activities at cSTART are based on different operation modes and ring lattice is flexible. DBA optics with achromatic straight sections will be applied for commissioning as well as for operation with large energy spread beams [11, 12, 13].

Anticipated parameters of ultra-short electron bunches after LPA plasma cell to be accepted for circulation in the cSTART ring are provided in Table 1 [16-21].

Table 1: Parameters of electron bunch after plasma cell

Parameter	Values
Beam energy	40 to 90 MeV
Magnetic rigidity of a ring	0.30 T·m
Energy spread of main spike	1.2 % (rms)
Number of particles per pulse	$6 \times 10^6$ to $6 \times 10^9$
Charge per pulse	1 pC to 1 nC
Pulse width	1 fs to 100 fs
Pulse length	0.3 to 30 $\mu\text{m}$
Repetition rate of laser pulses	1 to $10 \text{ s}^{-1}$
Transverse beam size $\sigma_x$	5 $\mu\text{m}$ (rms)
Transverse divergence, $\sigma_x'$	2 mr (rms)
Beam emittance $\epsilon_{x,y}$	10 nm (rms)

## DEEP VARIATION OF MOMENTUM COMPACTION FACTOR

VCF experiment (VSF) allows to reduce momentum compaction factor from  $\alpha=1.5 \times 10^{-2}$  down to about  $10^{-6}$  at ultra-low- $\alpha$  operation. VCF set up includes three pole chicane composed of parallel plate bending magnets of equal magnetic length (marked as blue strips in Fig.1). Magnetic field of middle dipole is double the field of side bending magnets. Leaking of dispersion at azimuth of chicane dipoles is necessary for a VCF experiment.

The remarkable feature of our low- $\alpha$  lattice is a compensation of positive contribution of dispersion function by negative one without stretching of a ring lattice (Fig. 2), in contrary to other rings, see for example [22]. Moreover, the magnitude of dispersion is reduced from 0.6 m at DBA optics to about 0.3 m at low- $\alpha$  [13]. At the same, efficiency of reduction of second term of compaction factor  $\alpha_2$  by

sextupoles is proportional to third power of the dispersion function  $D_0^3$  [1, 8]

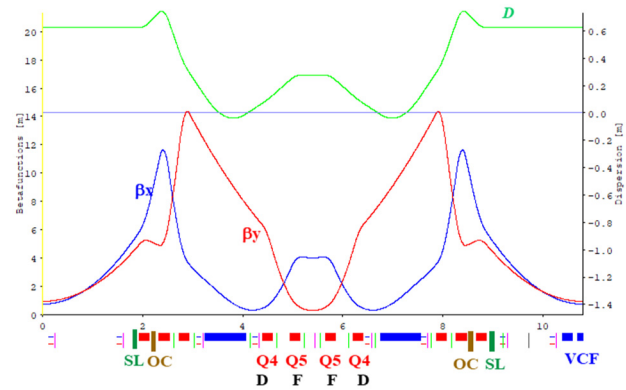


Figure 2: Lattice of one cell of a ring at low- $\alpha$  optics ( $\alpha=2 \times 10^{-4}$ ). Horizontal betatron function is marked by blue, vertical  $\beta$ -function – by red, dispersion function leaking into straights – by green.  $45^\circ$  bends shown as blue strips, quads – as red blocks, sextupoles – as green strips.

$$\Delta\alpha_2 = -\frac{1}{2L_0} \oint D_0^3 \cdot \Delta K_{SXT} ds \quad (8)$$

We choose DFFD sequence of Q4-Q5-Q5-Q4 quadrupoles at dispersive part of DBA cell (Fig. 2) to increase value of dispersion at straight from 0.3 to 0.6 m and limit strength of the sextupole family S1 incorporated in a ring lattice to control second term of momentum compaction factor.

The VCF experiment is planned in few steps. First, the ring lattice is tuned to low compaction factor optics with  $\alpha \approx 2 \times 10^{-4}$ . The leakage of dispersion function to all straights (Fig. 2) satisfies requirement described by formula (8).

Second, five families of sextupole magnets are tuned to minimize transverse chromaticity to slightly positive level of  $\xi_{x,y} \approx +0.2$ . Chromaticity should be precisely controlled during experiment to minimize bunch elongation due to amplitude dependent orbit lengthening (ADOL) [15].

Third, dedicated family of S1 sextupoles reduces longitudinal chromaticity stepwise while other five families of sextupoles are adjusted at each step to keep transverse chromaticity unchanged. To limit strength of S1 sextupoles at reasonable level we locate sextupole magnets at the beginning of straight sections as close as possible to maximum level of horizontal betatron function (Fig. 2).

Fourth, at positive  $\alpha_1 > 0$  octupoles are tuned to reverse the negative curvature of momentum compaction factor to positive value ( $\alpha_3 > 0$ ) and vice-versa at negative  $\alpha_1 < 0$ .

Fifth, when ring optics is fixed at optimum conditions the bending angle of the VCF chicane is increased stepwise to  $1.535^\circ$  to reduce momentum compaction factor further down to about  $10^{-6}$  [23]. Linear optics of ring (quadrupoles) is unchanged during VCF experiment while sextupoles are adjusted to minimize transverse and longitudinal

chromaticity. Ultra-short bunches are injected directly into a ring tuned for ultra-low- $\alpha$  optics.

Crossing zero value of synchrotron tune by off-momentum particles is considered as source of instability and beam loss [15, 22]. Variation of synchrotron frequency as function of energy deviation in a bunch is shown in Fig. 3. At low- $\alpha$  optics and uncontrolled longitudinal chromaticity the second term  $\alpha_2$  of momentum compaction factor is strong. As a result, the momentum acceptance of ring is limited and further reduction of compaction factor cannot be realized due to high slope of  $\alpha$ , see curve 1 in Fig. 3a. Applying family of “longitudinal” sextupoles S1 one could flatten the slope (curve 2 in Fig. 3b), restore momentum acceptance to reasonable level and improve lifetime of a beam.

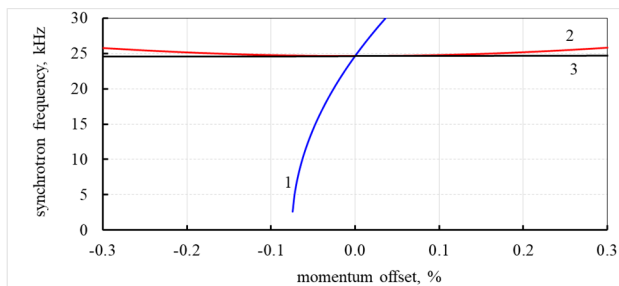


Figure 3: Synchrotron frequency as function of momentum offset. low- $\alpha$  optics with  $\alpha_1=2\times 10^{-4}$ , beam energy 90 MeV and RF voltage 500 kV. The curve (1) corresponds to  $\alpha_2=+0.13$  and  $\alpha_3=-0.145$ , curve (2) – reduced slope with  $\alpha_2=+1.07\times 10^{-5}$  and  $\alpha_3=+0.697$ , curve (3) – with same slope and reduced curvature  $\alpha_3=+1.2\times 10^{-3}$ . Beam is stable.

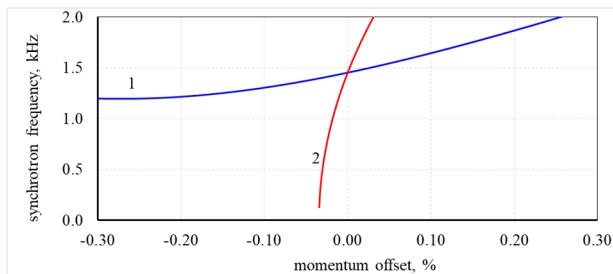


Figure 4: Synchrotron frequency as function of momentum offset at ultralow- $\alpha$  operation with  $\alpha_1=7\times 10^{-7}$ . The curve (1) corresponds to suppressed slope with  $\alpha_2=+8\times 10^{-5}$  and positive curvature  $\alpha_3=+0.01$ ; curve (2) – “natural” slope with  $\alpha_2=+1\times 10^{-3}$ .

Without tight control of high order terms of  $\alpha$  one can’t reduce momentum compaction factor further down. At ultralow- $\alpha$  operation with  $\alpha_1=7\times 10^{-7}$  “longitudinal” sextupoles S1 precisely flatten the slope of synchrotron tune by suppressing the second term of momentum compaction factor to  $\alpha_2=+8\times 10^{-5}$ . Momentum acceptance for off-momentum particles in a bunch is restored, see curve 1 in Fig.4. Even at reduced slope with  $\alpha_2=+1\times 10^{-3}$  the area of stability for off-momentum particles is shrunk to zero and ultra-short bunches will be lost, see curve 2 in Fig. 4.

Tight control and suppression of high order terms of momentum compaction factor are basic conditions for the VCF experiment. On- and off-momentum dynamic aperture of ultralow- $\alpha$  lattice is sufficient for circulation of ultra-short bunches in a ring.

Orbit length deviation for off-momentum particles at ultralow- $\alpha$  lattice with  $\alpha_1=7\cdot 10^{-7}$  is shown in Figure 5. Orbit length deviation is less than  $0.2\ \mu\text{m}$  (0.7 fs) for particles at periphery of energy distribution ( $\delta_E=\pm 0.3\%$ ). Zero current bunch length at ultralow- $\alpha$  operation mode and RF voltage of 500 kV is about 70 fs ( $21\ \mu\text{m}$ ) for expected energy spread of particles  $10^{-3}$  (formula 6). Contribution of finite dimensions of bunch in transverse planes leads to elongation of short pulses [24].

For a bunch of 10 nm rms emittance the contribution of dispersion integral  $H$  into bunch length is equivalent to 63 fs ( $19\ \mu\text{m}$ ). Total bunch length would be about 85 fs ( $28\ \mu\text{m}$ ). The coherent synchrotron radiation (CSR) will generate significant growth of energy spread of particles at bending magnets and pulse elongation until the bunch length will exceed wavelength of the CSR radiation [25, 26].

The bunch will circulate at non-equilibrium conditions and one will observe adiabatic growth of beam dimensions due to multiple intra-beam scattering of electrons (IBS) [27] as well as scattering of beam on atoms and molecules of residual gas [28]. Growth rate of beam emittance is varied from  $0.12\ \text{s}^{-1}$  for low intensity beam to  $12\ \text{s}^{-1}$  for initially high current bunch. The repetition rate of injection cycles of post-LPA bunches up to 10 Hz fits to abovementioned conditions.

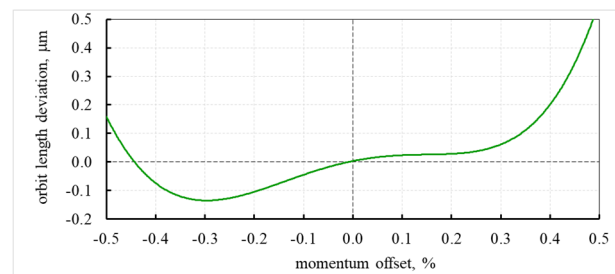


Figure 5: Orbit length deviation for off-momentum particles at ultralow- $\alpha$  operation where  $\alpha_1=7\cdot 10^{-7}$  and high order terms are suppressed to minimize bunch length and provide sufficient momentum acceptance. Bunch elongation is less than  $0.2\ \mu\text{m}$  (0.7 fs) for particles at periphery of energy distribution  $\delta_E=\pm 0.3\%$  ( $\delta_p=0.1\%$  rms).

## CONCLUSION

Extensive program of ARD experiments at ring is under development. LPA beam lines, experiments with ultra-short bunches of post LPA electrons, circulation of wide momentum spread beams, studies on inversed free electron laser and optical stochastic cooling. Flexible lattice of a ring with variable momentum compaction factor set up will benefit research program at cSTART.

## REFERENCES

- [1] A. Papash *et al.*, “Alpha-buckets in high energy electron storage rings (review of existing experiments and feasibility studies for future developments)”, *Adv. Theo. Comp. Phys.*, vol. 4, pp. 148-178, 2021. doi:10.5445/IR/1000139446
- [2] A.-S. Müller and M. Schwarz, “Accelerator based THz radiation sources”, *Synchrotron light sources and free electron lasers*, Springer international Switzerland, pp. 83-118, 2016. doi:10.1007/978-3-319-14394-1\_1
- [3] David A. G. Deacon, “Basic theory of the isochronous storage ring laser”, *Nuclear Instr. Methods*, vol. 76, pp. 349-391, 1981. doi:10.1016/0370-1573(81)90137-X
- [4] M. Attal, P. Brunelle, A. Loulergue, A. Nadj, L. Nadolski, M.-A. Tordeux, “Dynamics of three simultaneously stored beams in a storage ring”, *Phys. Rev. Accel. Beams*, vol. 16, p. 054001, 2013. doi:10.1103/PhysRevAccelBeams.16.054001
- [5] H. Wiedermann, “Higher order phase focusing”, in *Particle Accelerator Physics*, Fourth edition, Berlin, Heidelberg, Springer, pp. 289-302, 2015. doi:10.1007/978-3-319-18317-6
- [6] J-P. Delahaye, J. Jaeger “Variation of the dispersion function, momentum compaction factor, and damping partition numbers with particle energy deviations”. *Part. Acc.*, vol. 18, pp. 183-201, 1986.
- [7] A. W. Chao, K. Hubert Mess, M. Tigner and F. Zimmermann, “Nonlinear dynamics” in *Handbook of accelerator physics and engineering*, World Scientific, Second edition, 2013. doi:10.1142/8543
- [8] D. Robin, E. Forest, S. Pellegrini and A. Amiry, “Quasi-isochronous storage rings”, *Phys. Rev. E*, vol. 48, pp.2149-2156, 1996. doi:10.1103/Phys.RevE.48.2149
- [9] K.-Y. Ng, “Quasi-isochronous buckets in storage rings”, *Nucl. Instrum. Methods Sect. A*, vol. 404, pp. 199-216, 1998. doi:10.1016/S0168-9002(97)01136-4
- [10] A. Nadj, P. Brunelle, G. Flynn, M. P. Level, M. Sommer and H. Zygier, “Quasi-isochronous experiments with the Super-ACO storage ring”, *Nucl. Instrum. Methods*, A378, pp. 376-382, 1996. doi:10.1016/0168-9002(96)00415-9
- [11] A. Papash, E. Bründermann, and A.-S. Müller, “An optimized lattice for a very large acceptance compact storage ring”, in *Proc. 8th Int. Particle Accelerator Conf. (IPAC'17)*, Copenhagen, Denmark, May 2017, pp. 1402-1405. doi:10.18429/JACoW-IPAC2017-TUPAB037
- [12] A. Papash, E. Bründermann, A.-S. Müller, R. Ruprecht, and M. Schuh, “Design of a Very Large Acceptance Compact Storage Ring”, in *Proc. 9th Int. Particle Accelerator Conf. (IPAC'18)*, Vancouver, Canada, Apr.-May 2018, pp. 4239-4241. doi:10.18429/JACoW-IPAC2018-THPMF071
- [13] A. Papash *et al.*, “Modified lattice of a compact storage ring”, in *Proc. 12th Int. Particle Accelerator Conf. (IPAC'21)*, Campinas, SP, Brazil, 2021, pp. 159-162. doi:10.18429/JACoW-IPAC2021-MOPAB035
- [14] A. Papash *et al.* “Flexible features of the compact storage ring in the cSTART project at Karlsruhe Institute of Technology”, in *Proc. 13th Int. Particle Accelerator Conf. (IPAC'22)*, Bangkok, Thailand, 2022, pp. 2620-2623. doi:10.18429/JACoW-IPAC2022-THPOPT023
- [15] M. Ries, “Nonlinear momentum compaction and coherent synchrotron radiation at the Metrology Light Source”, *Ph.D. thesis*, Faculty of Mathematics and Natural Sciences, Humboldt University, Berlin, Germany. 2014. doi:10.18452/16979
- [16] T. Tajima and J. M. Dawson, “Laser electron accelerator”, *Phys. Rev. Lett.*, vol. 43, pp.267-270, 1986. doi:10.1103/PhysRevLett.43.267
- [17] H. T. Lim *et al.*, “Stable multi-GeV electron accelerator driven by waveform-controlled PW laser pulses”, *Sci. Rep.*, vol. 7, Aug. 2017, Art. No. 10203. doi:10.1038/s41598-017-09267-1
- [18] E. Brunetti *et al.*, “Low emittance, high brilliance relativistic electron beam from a laser-plasma accelerator”, *Phys. Rev. Lett.*, v. 105, 215007, Nov. 2007. doi:10.1103/PhysRevLett.105.215007
- [19] W. Lu *et al.*, “Generating multi-GeV electron bunches using single stage laser wakefield acceleration in a 3D nonlinear regime”, *Phys. Rev. ST Accel. Beams* 10, 06301. 2007. doi:10.1103/Phys.RevSTAB.10.061301
- [20] P. Antici *et al.*, “Laser-driven electron beamlines generated by coupling laser-plasma sources with conventional transport systems”, *Journ. Appl. Phys.* 112, p. 044902. 2012. doi:10.1063/1.4740456
- [21] M. Migliorati, A. Bacci, C. Benedetti, E. Chiaroni, M. Ferrario, A. Mostacci, L. Palumbo, A. R. Rossi,, L. Serafini, and P. Antici, “Intrinsic normalized emittance growth in laser-driven electron accelerators”, *Phys. Rev. ST Accel. Beams* 16, 011302. 2013. doi:10.1103/PhysRevSTAB.16.011302
- [22] A. I. Papash *et al.*, “Application of three families of sextupoles at the KARA ring of Karlsruhe Institute of Technology”, in *Proc. 14th Int. Particle Accelerator Conf. (IPAC'23)*, Venice, Italy, 2023, pp.984-987. doi:10.18429/JACoW-IPAC2023-MOPM007
- [23] S. Lee *et al.*, “Low energy electron ring with tunable compaction factor”, *Rev. of Scient. Instr.* 78, 075107. 2007. doi:10.1063/1.2754393
- [24] A. W. Chao *et al.*, “Ultralow longitudinal emittance storage rings”, *Phys. Rev. ST Accel. Beams*, 24, 090701, 16 p., 2021. doi:10.1103/PhysRevAccelBeams.24.090701
- [25] S. A. Kheifets and B. Zotter. “Coherent Synchrotron Radiation, Wake Field and Impedance”. *CERN SL Report* 95-43 (AP). Geneva, Switzerland. 1995.
- [26] A. Novokhatski. “Coherent synchrotron radiation: theory and simulations”. SLAC-PUB-14893, 15 p. 2012.
- [27] M. Venturini. “Study of intra-beam scattering in low energy electron rings”. in *Proc. 19th Particle Accelerator Conf. (PAC'2001)*, Chicago, USA. June 2001, pp. 2961-2963.
- [28] J. Le Duff, “Current and current density limitation in existing electron storage rings”, *Nuclear Instr. Methods*, A239, Issue 1, pp.83-101, 1985. doi:10.1016/0168-9002(85)90702-8